Experiments on forming behaviour of the aluminium alloy AA6016

R. Norz[1]*, F. R. Valencia[2], S. Gerke[2], M. Brünig[2] and W. Volk[1]

[1] Technical University of Munich, Chair of Metal Forming and Casting, Garching, Germany

[2] Universität der Bundeswehr München, Institut für Mechanik und Statik, Neubiberg, Germany

*roman.norz@utg.de

Abstract. Investigation of the sheet metal formability is an important issue in the design of components. During metal forming different deformation histories occur which may cause various damage and failure mechanisms on the micro-level affecting the quality of products. Therefore, description of the material characteristics by means of a linear limit change curve is not sufficient because the remaining formability and the fracture processes also depend on deformation history. For this purpose the aluminium alloy AA6016 is systematically investigated in order to obtain their forming capability as well as the damage and fracture behaviour after complex deformation paths. Different uniaxial tests with various initially unloaded and preloaded specimens have been performed to identify the effect of the forming history, the loading direction and the stress state on the formability and the mechanical parameters of the investigated material. The results can be used to propose a critical ratio between the pre-strain and the change in loading direction from which on shear failure occurs instead of necking behaviour leading to the loss of formability.

1. Introduction

The forming history significantly influences the remaining formability of sheet metals. For instance, Graf and Hoshford [1] found, that significant pre-forming affects the remaining formability of the aluminium alloy EN AW 2004-T4. Bergström and Ölund [2] received similar results for an aluminium-killed steel (AK-steel) and the aluminium alloy EN AW 2036-T4. Werber et al. [3,4] investigated three different pre-forming states (uniaxial, plane-strain and biaxial) as well as multiple pre-forming heights up to 50 % of the linear Forming Limit Curve (FLC) of an EN AW 6014 and found a significant effect of the pre-forming on the FLC. All mentioned publications coincide, that the pre-forming height significantly influence the remaining formability as well as the pre-forming state (e.g. uniaxial or biaxial). The pre-forming and the strain history also influences the fracture mode of materials. Gerke et al. [5] applied the X0-specimen to determine the dependence of non-proportional loading paths on damage evolution and fracture behaviour of an aluminium alloy EN AW 6082 and indicated the significant influence of the strain history on the fracture behaviour. In continuation Brünig et al. [6] confirmed these results with the H-specimen. Besides its influence on damage evolution and fracture behaviour the pre-loading history affects remarkably the load-displacement curves, while the

final stresses are almost unaffected. Consequently, the different pre-forming states can change the failure as well as the force-displacement behaviour significantly. Uniaxial pre-forming can lead to more brittle behaviour in subsequent shear tests based on a change from shear dominated damage mechanisms to a more void-dominated failure modes. When conducting the reverse load change, namely pre-shear followed by an uniaxial tensile test, the damage behaviour is micro-shear-crack dominated. Next to the pre-forming state and level, also the loading direction of anisotropic sheet metals has a significant effect on the remaining formability and the failure mode. Volk et al. [7] analysed the influence of a change in loading direction for a micro-alloyed steel HC340LA in Nakajima experiments. A distinct interaction between pre-forming level and change in loading direction on the formability and failure mode is stated. Specimens with no change in loading direction show ductile necking behaviour, while changes in loading direction by 45° or 90° leads to a shear failure of the material with significant loss of formability under uniaxial stress states. Change in loading direction lead to a significant increase in void growth, resulting in shear fracture.

In this paper, the aluminium alloy EN AW 6016-T4 with an initial thickness of 1 mm is investigated. The material has been initially characterized by tensile, plane-strain and biaxial tests under different angles with respect to the initial rolling direction. To investigate the influence of the pre-forming height and changes in loading direction, Nakajima experiments with pre-formed specimens are conducted. After the experiments SEM pictures of the fracture surfaces are taken to visualise the dominant failure modes.

2. Experimental setup

The experiments for the initial characterization are carried out on a Zwick Z150 uniaxial testing machine. To ensure comparable results of all experiments the machine velocity has been adapted to ensure a strain rate of 0.004 1/s. This was done by using a Laserextensometer to measure the strain between the strain gauge length. The strain gauge length was set to 50 mm for the tensile tests and 30 mm for both plane-strain specimen geometries. The strain distribution at the other specimen surface have been extracted by digital image correlation (DIC) with the optical measurement system Aramis SRX, allowing its comparison with numerically obtained results. All experiments are conducted under 0°, 22.5°, 45°, 67.5° and 90° with respect to the rolling direction. The used geometries can be found in Figure 1.

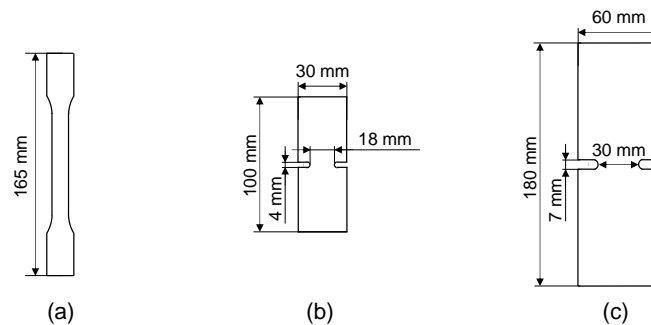**Figure 1.** Used specimen geometries, (a) tensile test, (c) 18 mm plane-strain specimen, (c) 30 mm plane-strain specimen

The initial Nakajima and bulge experiments are carried out on a Zwick BUP1000. The Nakajima experiments are conducted according to ISO12002-2 with a constant punch velocity of 1 mm/s. The frame rate for the optical measurement system Aramis 4M is set to 10 Hz and the onset of necking is determined by the Time Dependent Evaluation Method (TDEM) by Volk and Hora [8]. A total of nine different specimen widths under 0°, 45° and 90° to the initial rolling direction are investigated, leading to a total of 25 data points corresponding to each other in all investigated directions. To reduce the friction between the punch and the specimen a PVC-pad with a thickness of 3 mm and lubrication paste

are applied. The consecutive forming of the pre-strained specimens is conducted in the same way as the initial Nakajima experiments using four different specimen widths. The chosen specimen widths are 30 mm, 100 mm, 130 mm and 235 mm for the biaxial specimen. For all experiments at least three valid experiments are performed.

The pre-forming of the specimens has been realized on a hydraulic press using a modified Marciniak-tool, proposed by Weinschenk and Volk [9], a more detailed description of the tool can be found there. The punch speed is set to a constant value of 15 mm/s and the blank holder force is set to 1200 kN. In combination with the drawbead, the material flow is impeded. To allow high uniaxial pre-forming heights, the specimen geometry, as shown in Figure 2 (b), is used. The reduced width in the center of the specimen, where the punch is in contact with the specimen, ensures that the main deformation occurs there. To minimize a possible deviation in the pre-forming levels and pre-forming states an incremental pre-forming process is chosen. After a certain displacement the specimens will be re-lubricated with deep drawing oil to minimize the influence of friction on the results. The used tool, the specimens geometry and the process to change the loading direction are shown in Figure 2. The sample designation IF stands for the initial pre-forming direction, while PF stands for the post-forming direction. The introduced strains of the pre-forming process are measured by GOM Argus. A total of three different pre-forming levels, approximately 25 %, 35 % and 50 % of the linear FLC, are taken into account.
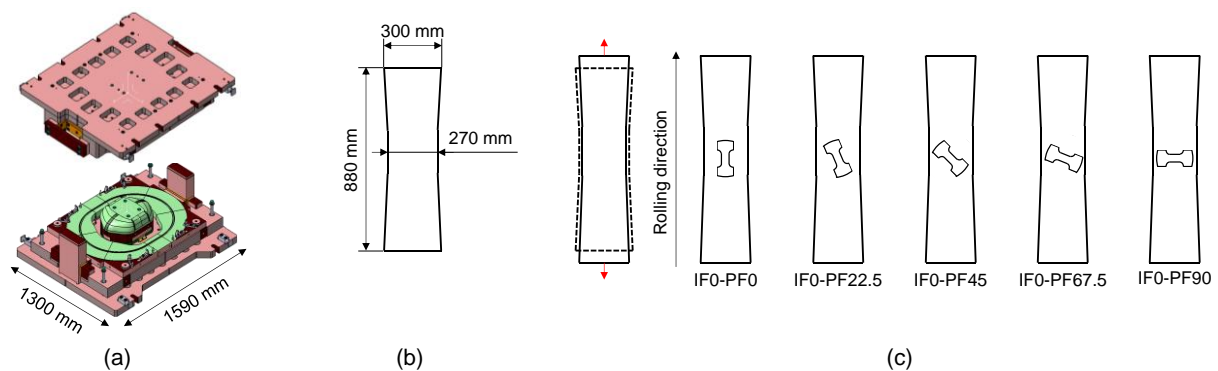

Figure 2. (a) Marciniak tool used to pre-form the specimens, (b) specimen geometry and (c) specimen extraction and nomenclature.

3. Results

3.1. Initial experiments

The tensile and plane strain tests indicated only a small material influence of the loading direction on the force-displacement curves, see Figure 3 (a) and (b). The force-displacement curve of the plane-strain specimen with a width of 18 mm the lower ones in Figure 3 (b) due to the smaller cross-section. It is also noted, that the deviation between the specimens is very small. The influence of the angle with respect to the rolling direction on the formability i.e. the Forming Limit Curves (FLC), is indicated in Figure 3 (c). The FLC under 0° with respect to the rolling direction displays the lowest formability under all investigated strain states. For the uniaxial Nakajima specimens with 30 mm width, brittle shear fracture was observed, the major strain distribution can be found in Figure 5 (a).
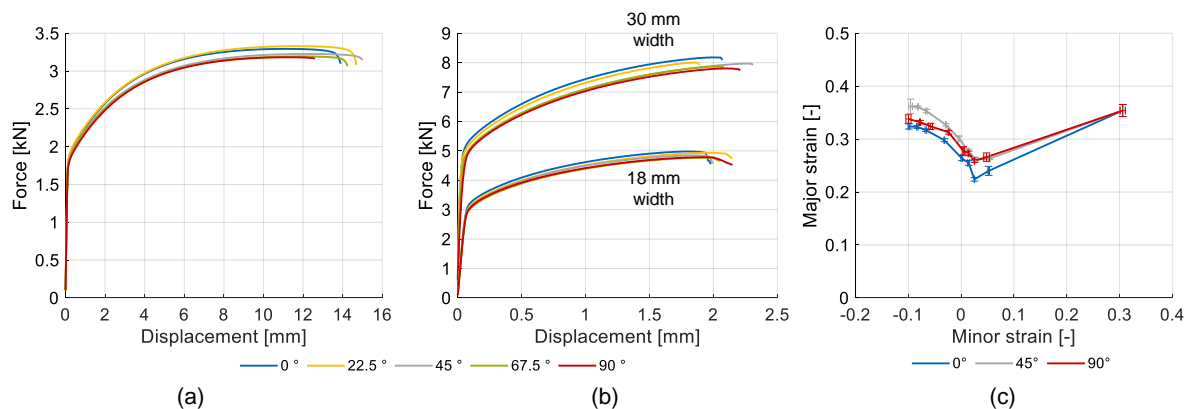
Figure 3. (a) Force-Displacement curves from tensile test, (b) force-displacement curves for the 18 mm plane-strain and the 30 mm plane-strain specimens and the (c) forming limit curve for different angles with regard to the rolling direction.

The Lankford-coefficients and their variation under different angles with regard to the initial rolling direction can be found in Table 1.

Table 1. Lankford-coefficients under different angles with respect to the initial rolling direction.

$r_{0°}$	$r_{22.5°}$	$r_{45°}$	$r_{67.5°}$	$r_{90°}$
0.672	0.593	0.464	0.529	0.611

All those experiments are used to determine and to optimize the yield criterion for this material. Best results could be obtained for the YLD2000-2d criterion by Barlat et al. [10]. The final determination of parameters has been realized by an inverse optimization procedure using the experiments used to characterize the material and was conducted with LS-Dyna using the R11.2.1 solver with double precision. As for example the plane-strain specimens or the tensile test under 22.5° and 67.5° are not used in the calibration process of the YLD2000-2d model and can therefore be used for the optimization. The optimization was done in LS-Dyna. The optimized material parameters, given in Table 2, are used in future numerical investigations of the experiments.

Table 2. Values for the YLD2000-2d model.

α_1	α_2	α_3	α_4	α_5	α_6	α_7	α_8	m
0.9764	0.9705	0.8999	1.0234	1.0249	1.0348	0.9452	0.1279	7

3.2. Pre-formed Nakajima experiments

The pre-formed Nakajima experiments reveal an influence of the loading direction on the formability of the material. The higher the pre-forming, the more a change in loading direction influences the remaining formability. Where all investigated post-forming angles show similar remaining formability for the 25 % pre-forming, the IF0°-PF45° and IF0°-PF90° are below the IF0°-PF0° curve for the 50 % pre-forming under uniaxial stress state, using the specimen with a specimen width of 30 mm. Therefore, a change in loading direction does influence the remaining formability in the uniaxial stress state. For all other specimen geometries, 100 mm, 130 mm and 235 mm, only a small effect can be observed, see Figure 4. Compared to the results of Volk et al. [11] for the micro-alloyed steel HC340LA the influence is less pronounced. This is possibly caused by the fact that the fracture curve, where the first crack in the specimen occur, and the forming limit curve, where necking begins, are close to each other and

therefore only limited sliding is possible before the specimen shows the first cracks. This is not the case for the HC340LA steel, where the material can be further deformed after the onset of necking until the first cracks occur. A closer look on the experimental FLC indicates, that the uniaxial specimens stagnate in the major strains. This is caused by the non-linearity of the strain path in the experiment. When the pre-formed Nakajima experiments under a uniaxial stress state are conducted, the onset of necking is far beyond the linear FLC. The strain path has been linearized by the methodology of Volk and Gaber [12]. After linearization, the initial experimental FLC is in good agreement with the FLCs obtained from pre-formed experiments.
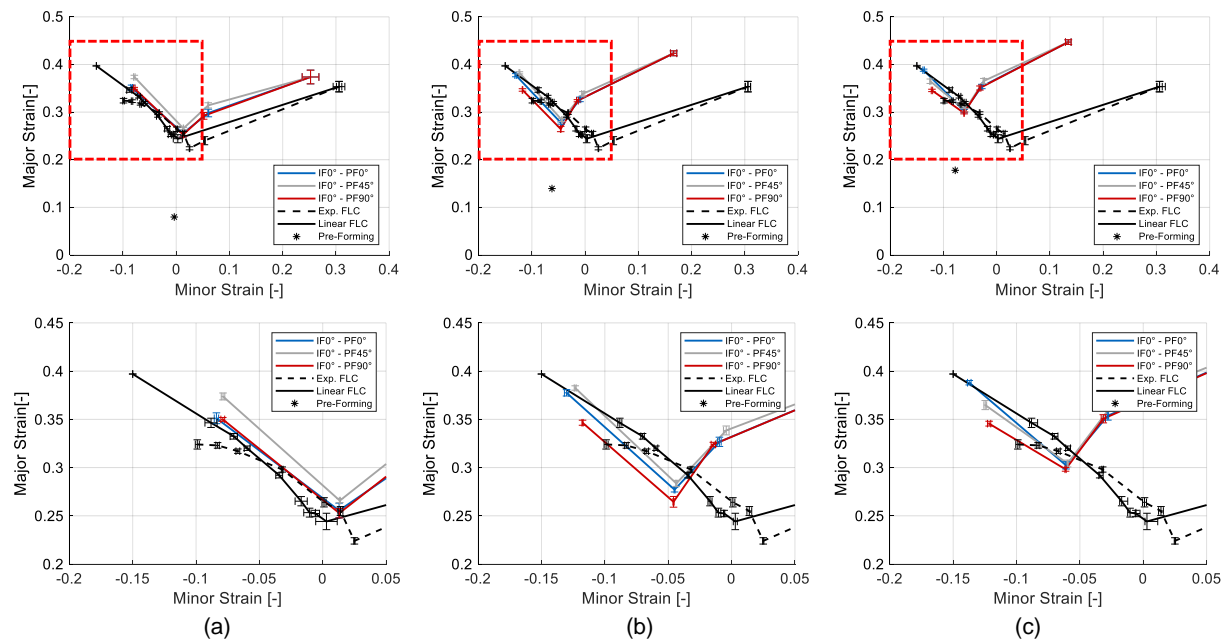

Figure 4. Forming Limit Curves for the three pre-forming levels, (a) 25 % of the linear FLC, (b) 35 % of the linear FLC and (c) 50 % of the linear FLC. The areas in the red-square are plotted in the lower figures with a higher resolution.

It is also found, that the failure mode has altered after the change in loading direction of 90° (IF0-PF90) and the pre-forming of 50 % of the linear FLC. While the initial material and the material with no change in loading direction (IF0-PF0) indicate a shear failure behaviour, the IF0-PF90 specimens show ductile failure behaviour with a necking zone in the middle of the specimens. This can be seen in contrast to the material behaviour of the HC340LA, where the initial material and the IF0-PF0 specimens revealed ductile failure behaviour in the centre of the specimens and the IF0-PF90 specimens showed brittle shear failure behaviour. DIC pictures of the major strain distribution for the initial specimen under 0° with respect to the rolling direction, a IF0-PF0 specimen and a IF0-PF90 specimen before fracture can be seen in Figure 5.
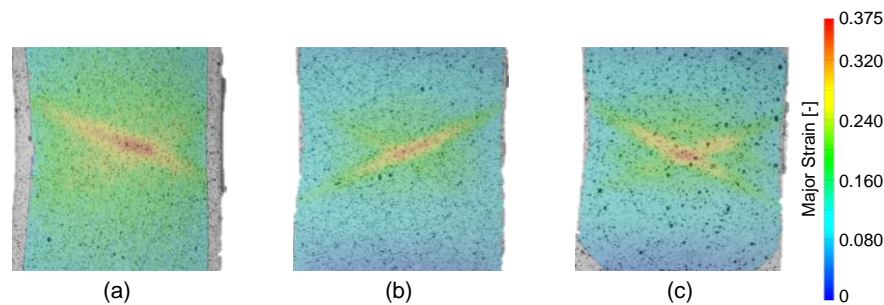
Figure 5. Major strain distribution at the stage before crack of the (a) initial 0° uniaxial Nakajima specimen, (b) of the IF0-PF0 uniaxial Nakajima specimen with a pre-forming of 50 % and (c) of the IF0-PF90 uniaxial Nakajima specimen with a pre-forming of 50 %.

Using scanning electron microscopy (SEM), fracture surfaces from Nakajima experiments with pre-formed specimens were analysed. The SEM images reveal that the IFO-PF90 fracture surface experiences ductile extrusion failure modes manifested in the greater detachment of material in the matrix, as observed in Figure 6 (c) (red circle). In addition, the generation of higher number of voids should have led to earlier failure as observed in the tension and plane strain tests, observed in Figure *3* (a) and (b). On the other hand, micrographs of the initial 0° uniaxial Nakajima experiments (Figure 6 (a)) and the pre-formed Nakajima experiments IF0-PF0, in Figure 6 (b) show similar behaviour. The fracture surfaces show stretched and oval voids, which means that the failure mode of the material was due to a sudden shear failure without any prior necking. The reason for these behaviours will be addressed in future work during this project.
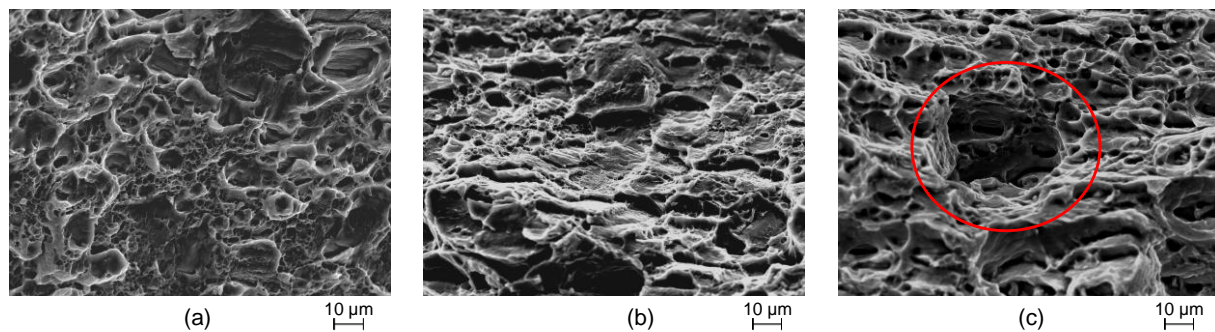

Figure 6. (a) Fracture surface of an initial 0° uniaxial Nakajima specimen, (b) fracture surface of a IF0-PF0 uniaxial Nakajima specimen and (c) fracture surface of a IF0-PF90 uniaxial Nakajima specimen.

4. Conclusion and Outlook

The material AA6016-T4 has been investigated in this paper, regarding the influence of uniaxial pre-forming on the remaining formability. It is found, that changes in loading direction influences the failure mode of the material after a pre-forming of 50 % of the linear FLC. The failure mode changes from brittle shear fracture to ductile necking fracture. Nevertheless, reduced formability can be observed, but is not as significant as for the HC340LA investigated in [11]. To determine the influence of different pre-forming states, also plane-strain pre-formed Nakajima experiments are planned. Next to the experimental investigations, a numerical damage model will be developed which should be able to capture the anisotropic damage behaviour of the investigated material. This model will give more information on the occurring stress states and damage mechanisms leading to the different fracture modes.

Acknowledgement

References

[1] Graf A. and Hosford W. 1993 Effect of Changing Strain Paths on Forming Limit Diagrams of AI 2008-T4. *Metall Mater Trans A* **24:**671. DOI: 10.1007/BF02646529

[2] Bergström Y. and Ölund S. 1982 The forming limit diagram of sheet metals and effects of strain path changes on formability: a dislocation treatment. *Materials Science and Engineering* **56:**47–61. DOI: 10.1016/0025-5416(82)90181-1

[3] Werber A., Liewald M., Nester W., Grünbaum M., Wiegand K., Simon J., Timm J., Bassi C. and Hotz W. 2012 Influence of Different Pre-Stretching Modes on the Forming Limit Diagram of AA6014. *KEM* **504-506:**71–76. DOI: 10.4028/www.scientific.net/KEM.504-506.71

[4] Werber A., Liewald M., Nester W., Grünbaum M., Wiegand K., Simon J., Timm J. and Hotz W. 2013 Assessment of forming limit stress curves as failure criterion for non-proportional forming processes. *Prod. Eng. Res. Devel.* **7:**213–221. DOI: 10.1007/s11740-013-0446-6

[5] Gerke S., Zistl M. and Brünig M. 2020 Experiments and numerical simulation of damage and fracture of the X0-specimen under non-proportional loading paths. *Engineering Fracture Mechanics* **224:**106795. DOI: 10.1016/j.engfracmech.2019.106795

[6] Brünig M., Zistl M. and Gerke S. 2021 Numerical Analysis of Experiments on Damage and Fracture Behavior of Differently Preloaded Aluminum Alloy Specimens. *Metals* **11:**381. DOI: 10.3390/met11030381

[7] Volk W., Norz R., Eder M. and Hoffmann H. 2020 Influence of non-proportional load paths and change in loading direction on the failure mode of sheet metals. *CIRP Annals* **69:**273–276. DOI: 10.1016/j.cirp.2020.03.009

[8] Volk W. and Hora P. 2011 New algorithm for a robust user-independent evaluation of beginning instability for the experimental FLC determination. *Int J Mater Form* **4:**339–346. DOI: 10.1007/s12289-010-1012-9

[9] Weinschenk A. and Volk W. 2017 FEA-based development of a new tool for systematic experimental validation of nonlinear strain paths and design of test specimens. *AIP Conference Proceedings* **1896**. DOI: 10.1063/1.5007966

[10] Barlat F., Brem J.C., Yoon J.W., Chung K., Dick R.E., Lege D.J., Pourboghrat F., Choi S.-H. and Chu E. 2003 Plane stress yield function for aluminum alloy sheets—part 1: theory. *International Journal of Plasticity* **19:**1297–1319. DOI: 10.1016/S0749-6419(02)00019-0

[11] Volk W., Gruber M. and Norz R. 2020 Prediction of limit strains during non-proportional load paths with a change in loading direction. *IOP Conf. Ser.: Mater. Sci. Eng.* **967:**12069. DOI: 10.1088/1757-899X/967/1/012069

[12] Volk W. and Gaber C. 2017 Investigation and Compensation of Biaxial Pre-strain During the Standard Nakajima- and Marciniak-test Using Generalized Forming Limit Concept. *Procedia Engineering* **207:**568–573. DOI: 10.1016/j.proeng.2017.10.1022